

Design and implementation of fast output sampling feedback control for shape memory alloy actuated structures

K. Dhanalakshmi¹, M. Umapathy*¹, D. Ezhilarasi¹ and B. Bandyopadhyay²

¹*Department of Instrumentation and Control Engineering, National Institute of Technology,
Tiruchirappalli - 620 015, India*

²*Systems and Control Engineering, Indian Institute of Technology Bombay, Mumbai - 400076, India*

(Received July 16, 2009, Revised June 29, 2011, Accepted July 20, 2011)

Abstract. This paper presents the design and experimental evaluation of fast output sampling feedback controller to minimize structural vibration of a cantilever beam using Shape Memory Alloy (SMA) wires as control actuators and piezoceramics as sensor and disturbance actuator. Linear dynamic models of the smart cantilever beam are obtained using online recursive least square parameter estimation. A digital control system that consists of Simulink™ modeling software and dSPACE DS1104 controller board is used for identification and control. The effectiveness of the controller is shown through simulation and experimentation by exciting the structure at resonance.

Keywords: shape memory alloy actuator; smart structure; system identification; active vibration control; fast output sampling feedback control.

1. Introduction

The increased demand for faster, quieter and more efficient lightweight mechanisms has resulted in unacceptable vibration levels in flexible mechanisms and structures. Vibrations affect the stability, increase noise level and reduce operating life due to fatigue wear of components. Design strategies to suppress the elastodynamic response of flexible structures are a main concern in the field of vibration control. Active damping involves sensing the levels of vibration of the structure and applying appropriate control strategy to provide strategically located actuators with compensated commands to drive the vibration levels within desired limits (Srinivasan and McFarland 2001).

With recent advances in materials technology, smart materials such as piezoelectric materials, shape memory alloys (SMA) and electro-rheological (ER) fluids are playing an increasingly significant role in the active vibration control of flexible mechanisms. SMA such as Nickel-Titanium (Ni-Ti) wires, have the property of shortening when heated and thus are able to apply forces. This phenomenon called the Shape Memory Effect (SME) occurs when the material is heated above a certain transition temperature changing its crystalline phase from martensite to austenite. Heating, and thus actuation, of an SMA wire is easily accomplished by Joule heating. Other features that add credit to the application of SMA wires as actuators are their incredibly small size and weight, high force to weight ratio, simple design and noiseless operation. Its characteristic of small bandwidth finds

*Corresponding Author, Professor, E-mail: umapathy@nitt.edu

application in low frequency vibration control (as seen from Baz *et al.* 1990, Choi and Cheong 1996, Seelecke and Muller 2004, Sohn *et al.* 2009 and related references).

Unlike other smart materials, SMA wire actuators can produce high force for large displacement control system. Application of SMA for active vibration and position control has been under study since the last two decades. Baz *et al.* 1990 presented the application for vibration control of flexible beam with on-off controller. Choi *et al.* 1996 had later developed a more feasible structure to demonstrate vibration control using Amplitude Control and Sliding Mode Control. Sohn *et al.* 2009 have studied on vibration and position tracking control of a flexible beam using SMA wire actuators by formulating the Sliding mode control to account for robust control.

The choice of control technique is important in designing controllers which ensure the suitable functioning of flexible structures under required conditions and also can be easily implemented. Over the past decades, many advances have been made in the field of control theory and its application to structural control which rely on powerful tools of state-space theory. A feedback control technique that does not require any state information can be of immense help in many applications. Hence it is desirable to design a controller based only on the plant output. The static output feedback problem is one of the most investigated problems in control theory however, complete pole assignment and guaranteed closed-loop stability is not obtained. The dynamic output feedback controller involves more dynamics and is complex to design. Another approach to pole placement problem is to consider the potential of Multirate Output Feedback (MROF) control. MROF is the concept of sampling the control input and sensor output of system at different rates. MROF can guarantee closed loop stability, a feature not assured by static output feedback. At the same time the structural simplicity of static output feedback is maintained in MROF. Fast Output Sampling (FOS) feedback is a kind of MROF in which the system output is sampled at a faster rate as compared to the control input as proposed by Werner and Furuta 1995, Ezhilarasi *et al.* 2006. In this paper, a fast output sampling feedback controller is designed and implemented for the vibration control of SMA actuated cantilever beam.

The organization of this paper is as follows: in section 2, the experimental set up of the smart structure employed for identification and control is described. The recursive identification method used to identify the dynamic model of the structure and the obtained system models are given in Section 3. A brief review of the FOS control law is given in Section 4. Controller designs and simulation results are reported in Section 5. The experimental implementation and results are presented in Section 6, followed by the conclusions in Section 7.

2. The experimental system

In order to verify the effectiveness of vibration control strategies, the experimental setup shown in Fig. 1(a) is designed and built. The setup consists of the following three main parts: i) the beam under test with the PZT elements bonded to its surface and externally connected SMA wire actuators and, the fixture ii) the instrumentation setup - a charge amplifier and a voltage amplifier for the PZT sensor and disturbance actuator, current amplifiers for the SMA wire actuators and the data acquisition board iii) the software interface - the visuals and the control algorithm to process the measured signal and issue the appropriate control signal.

A clamped-free aluminum beam fixed vertically along its width is considered in this work. Two collocated piezoceramic patches are surface bonded at a distance of 8 mm from the fixed end; the

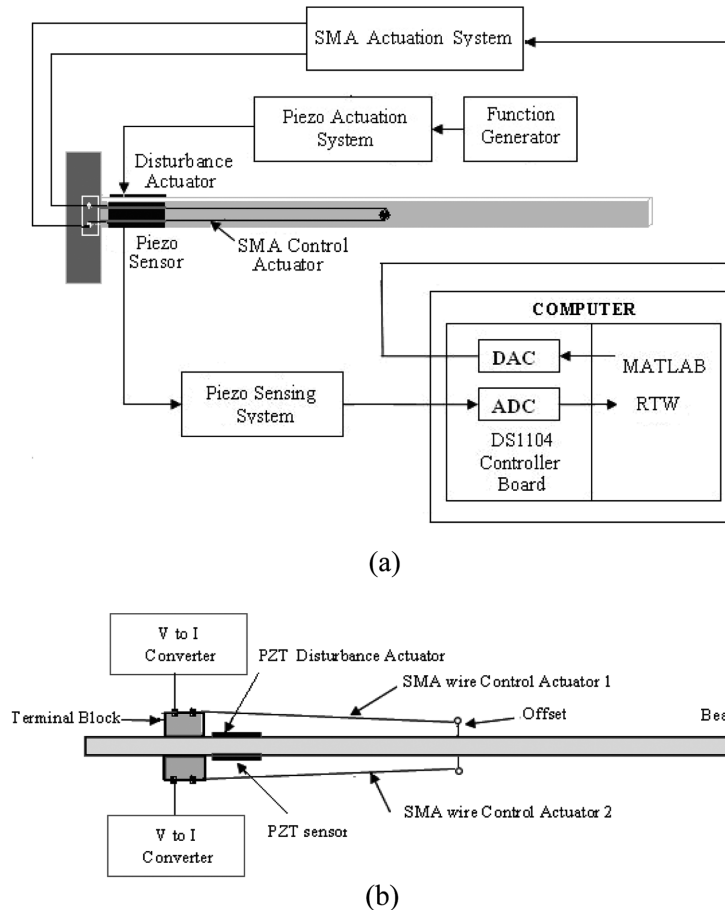


Fig. 1 Experimental setup (a) Schematic diagram and (b) Actuator/sensor location

beam is excited using one piezoceramic patch and the response is sensed using another. Symmetrically mounted antagonistic pair of SMA (NiTiNOL) wires is attached externally to the beam on both sides to function as control actuators. The dimensions and material properties of the beam, piezoceramic patches and NiTiNOL wires are listed in Table 1, Table 2 and Table 3 respectively. PZT (Lead Zirconate Titanate) of type SP-5H which is equivalent to NAVY TYPE VI, the product from Sparkler Ceramics Pvt. Ltd. India are used as the sensor and disturbance actuator. Nitinol wires under the trade name Flexinol® procured from Dynalloy Inc., USA are designed and used as control actuators. Flexinol is a binary alloy (Ni-Ti: 50.5-49.5%) with a one-way shape memory effect. The arrangement of Nitinol wire actuators is shown in Fig. 1(b). On each side of the beam a NiTi SMA wire (90C Flexinol) is strung between two terminal points at the fixed end of the beam and a stub with an offset, anchored at the midpoint of the beam creating two 56.5 cm parallel lengths of wire. In effect each SMA wire is electrically single while it forms two mechanically parallel wires in equivalent. This provides ease of electrical connection to the SMA wires. Such mechanically parallel but electrically serial wires provide the benefit of producing high output force. The usage of two actuator wires allows their alternate heating and cooling thereby permitting continuous actuation through joule heating. Current through them is routed by software switching,

Table 1 Dimensions and properties of the aluminum beam

| | | |
|-------------------------------|----------|---------|
| Length (m) | l_b | 1.1 |
| Width (m) | b_b | 0.0254 |
| Thickness (m) | t_b | 0.00316 |
| Young's Modulus (GPa) | E_b | 76 |
| Density (kg/m ³) | ρ_b | 2962.3 |
| First Natural Frequency (Hz) | f_1 | 2.13 |
| Second Natural Frequency (Hz) | f_2 | 13.39 |

Table 2 Dimensions and properties of the piezoceramic sensor/actuator

| | | |
|--|----------|------------------------|
| Length (m) | l_p | 0.0762 |
| Width (m) | b_p | 0.0254 |
| Thickness (m) | t_p | 0.001 |
| Young's Modulus (GPa) | E_p | 47.62 |
| Density (kg/m ³) | ρ_p | 7500 |
| Piezoelectric Strain Constant (m V ⁻¹) | d_{31} | -247×10 ⁻¹² |

Table 3 Dimensions and properties of the NiTiNOL wire actuator

| | | |
|---|------------|----------|
| Length (m) | l_s | 1.13 |
| Diameter (m) | d_s | 0.000127 |
| Transition Temperature (°C) | T_t | 90 |
| Martensite Start Temperature (°C) | M_s | 72 |
| Martensite Finish Temperature (°C) | M_f | 62 |
| Austenite Start Temperature (°C) | A_s | 88 |
| Austenite Finish Temperature (°C) | A_f | 98 |
| Young's modulus (GPa) | | 28 |
| Martensite | E_M | 75 |
| Austenite | E_A | |
| Resistance (ohm/m) | R_s | 70.866 |
| Approximate Current at room temperature (A) | I_s | 0.25 |
| Contraction Time (s) | t_{cont} | 1 |
| Off Time (s) | t_{off} | 0.9 |
| Maximum Pull Force (kg) | F_{max} | 0.230 |

so that RMS value of the positive current heats one wire and the RMS value of negative current commands the other. The locations of the sensor and the actuators have been selected for the best performance.

The excitation signal to the disturbance actuator is applied using an arbitrary waveform generator (Agilent 33220A). The sensor output signal is conditioned using a piezo sensing system and is given to the ADC input on the dSPACE DS1104 controller board. The control algorithm is developed using SimulinkTM software and implemented in real time on dSPACE DS1104, using RTW and dSPACE real time interface tools. The SimulinkTM software is used to build control block diagrams and real time workshop is used to generate C code from the SimulinkTM model. The C code is then converted to target specific code by real time interface and target language compiler

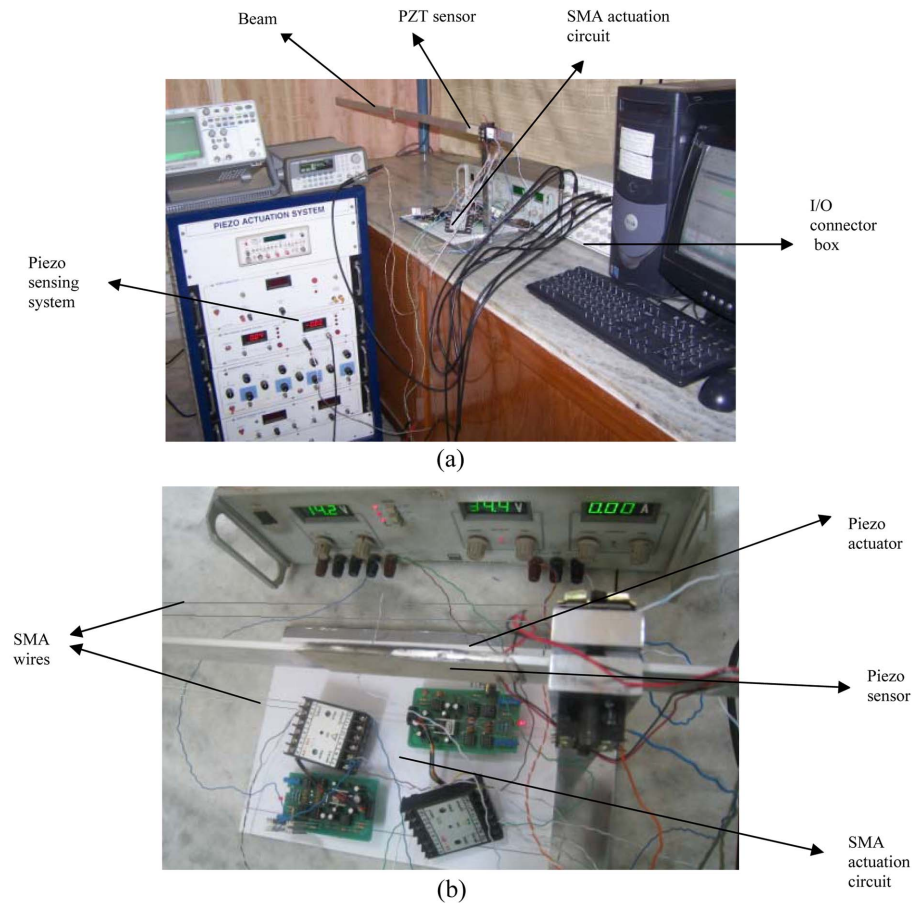


Fig. 2 Photograph of (a) the experimental setup and (b) structure with electronics

supported by dSPACE DS1104. This code is then deployed on to a rapid prototype hardware system, to run the hardware in the loop simulation. Control signal generated from SimulinkTM is interfaced to the SMA actuation system through DAC unit of dSPACE DS1104. The two DAC outputs from the DS1104 are connected to two current regulators which supply electrical power to the SMA wires. Each regulator is capable of delivering about 0.30 A to its load, which is sufficient to heat the SMA wire at room temperature. All real-time computation and data capture functions are performed on a DS1104 board from dSPACE. Photographs of the experimental setup are shown in Figs. 2(a) and (b). The SMA wires are too thin (0.1 mm diameter) to be visible in the photograph in Fig. 2(a).

3. Identification of the dynamics of the system

The linear dynamic model of SMA actuated cantilever beam is obtained using online Recursive Least Square (RLS) parameter estimation as in Ljung 1999 and Bu *et al.* 2003. The unknown parameters of the smart structure dynamics are estimated using online identification method, since it

is proven to be more universal and feasible than analytical and numerical models for the present system. In addition, the RLS method based on Auto-Regressive (ARX) model is used for linear system identification, which is easy to implement and has fast parameter convergence. Most multi-input single-output plants can be considered by the auto-regressive model.

The ARX model for the system shown in Fig. 1 is given as,

$$\begin{aligned} \hat{y}(k) + a_1 y(k-1) + \dots + a_{n_a} y(k-n_a) = & bl_1 u_1(k-1) + \dots + bl_{n_{b1}} u_1(k-n_{b1}) + b2_1 u_2(k-1) \\ & + \dots + b2_{n_{b2}} u_2(k-n_{b2}) + e_1 d(k-1) + e_{n_e} d(k-n_e) + d(k) \end{aligned} \quad (1)$$

where $u_1(k)$ and $u_2(k)$ are the input signals, $y(k)$ is the piezo sensor output, $e(k)$ is the disturbance input and n_a , n_{b1} , n_{b2} and n_e determine the model order. The vector of unknown parameter to be estimated is thus

$$\theta = [a_1 \ a_2 \ \dots \ a_{n_a}, bl_1 \ bl_2 \ \dots \ bl_{n_{b1}}, b2_1 \ b2_2 \ \dots \ b2_{n_{b2}}, e_1 \ e_2 \ \dots \ e_{n_e}]^T \quad (2)$$

Data vector φ calculated based on measured signals and known variables is given by

$$\begin{aligned} \varphi(k) = & (-y(k-1), -y(k-2), \dots, -y(k-n_a), u1(k-1), u1(k-2), \dots, u1(k-n_{b1}), \\ & u2(k-1), u2(k-2), \dots, u2(k-n_{b2}), d(k-1), d(k-2), \dots, d(k-n_e))^T \end{aligned} \quad (3)$$

The estimated model output is

$$\hat{y}(k) = \varphi^T(k) \hat{\theta}(k-1) \quad (4)$$

In recursive identification methods, the parameter estimates are computed recursively in time. The recursive form is given by

$$\hat{\theta}(k) = \hat{\theta}(k-1) + P(k) \varphi(k) \varepsilon(k) \quad (5)$$

where $P(k)$ is the covariance matrix which is updated using

$$P(k) = P(k-1) \left(1 - \frac{\varphi(k) \varphi^T(k) P(k-1)}{1 + \varphi^T(k) P(k-1) \varphi(k)} \right) \quad (6)$$

$$\varepsilon(k) \text{ is the prediction error and is given by } \varepsilon(k) = y(k) - \hat{y}(k) \quad (7)$$

The initial values of $\hat{\theta}(k)$ and $P(k)$ are chosen to be $\hat{\theta}(0) = 0$ and $P(0) = \alpha I_Z$ where $\alpha = 10^5$. The natural frequency of the structure is measured experimentally as 2.355 Hz. The first mode frequency of the structure is measured by sweeping the excitation signal frequency applied to disturbance actuator from zero until the resonance is observed. To identify the parameters online, the structure is excited by a sinusoidal signal through the disturbance actuator and a square wave signal as input to the control actuators. The disturbance signal is in the frequency range of 0 to 20 Hz which includes first two natural frequencies. Control actuator (SMA) 1 is excited for a period of

1 second and for the next 1 second control actuator 2 is actuated by the same square wave signal. The input-output data is then collected. The sampling time is set to provide approximately five measurements per cycle. The excitation signal, Root Mean Square (RMS) values of the input signals and sensor output are given to MATLAB/Simulink™ through Analog to Digital Converter (ADC) port of dSPACE 1104 system. The RLS algorithm is implemented by writing a C-file S-function be used with Real Time Workshop of MATLAB/Simulink™. The algorithm is run dynamically until all the parameter values settle down to a final steady value.

The models are identified to represent the first vibration mode (second order model) and the first two vibration modes (fourth order model). The continuous time state space model derived from the identified second order ARX model is

$$\dot{\mathbf{x}} = \mathbf{A}\mathbf{x} + \mathbf{b}u + \mathbf{E}d; y = \mathbf{C}^T\mathbf{x} \quad (8)$$

where \mathbf{A} is the system matrix, \mathbf{b}_1 and \mathbf{b}_2 are the control input matrices for actuator 1 and 2 respectively, \mathbf{E} is the disturbance input matrix and \mathbf{C}^T is the output matrix. The matrices of the second order model is

$$\mathbf{A} = \begin{bmatrix} 1.0264 & 5.3088 \\ -14.4770 & -1.5851 \end{bmatrix}, \mathbf{b}_1 = \begin{bmatrix} -0.083 \\ -0.358 \end{bmatrix}, \mathbf{b}_2 = \begin{bmatrix} -0.065 \\ -0.380 \end{bmatrix}$$

$$\mathbf{E} = \begin{bmatrix} -0.0369 \\ -0.1396 \end{bmatrix} \text{ and } \mathbf{C}^T = [1 \ 0] \quad (9)$$

This model has been validated and it is found that the mode frequency obtained from the identified model is 2.3379 Hz and is close to the experimentally measured mode frequency 2.36 Hz. In order to validate the model with time domain data the structure is excited with mixed mode frequency signal. Comparison of responses shown in Fig. 3 indicates close agreement of the model with the actual structure response. Validation is also carried out by studying the parameter convergence and it is found that the model parameters converge to specific values at about 20 s.

The identified matrices of the fourth order system model are given in Eq (10).

$$\mathbf{A} = \begin{bmatrix} -8.1014 & 44.0910 & -33.0069 & 44.8883 \\ -7.4318 & -15.8734 & 49.9091 & -40.9194 \\ 39.2611 & -48.8946 & 15.1660 & 7.6967 \\ -42.6148 & 31.9018 & -43.3854 & 7.6737 \end{bmatrix}, \mathbf{E} = \begin{bmatrix} -0.0186 \\ 0.1593 \\ -0.2509 \\ -0.0448 \end{bmatrix}$$

$$\mathbf{b}_1 = \begin{bmatrix} 0.1660 \\ -0.4495 \\ 0.2575 \\ 0.7325 \end{bmatrix}, \mathbf{b}_2 = \begin{bmatrix} 0.2155 \\ -0.4250 \\ 0.1940 \\ 0.8620 \end{bmatrix} \text{ and } \mathbf{C}^T = [1 \ 0 \ 0 \ 0] \quad (10)$$

The above model has also been validated and it is found that the mode frequency obtained from the identified model is 13.408 Hz and is close to the experimentally measured mode frequency 13.45 Hz. The estimated model parameters converge to their respective true values between 5 and 10 seconds.

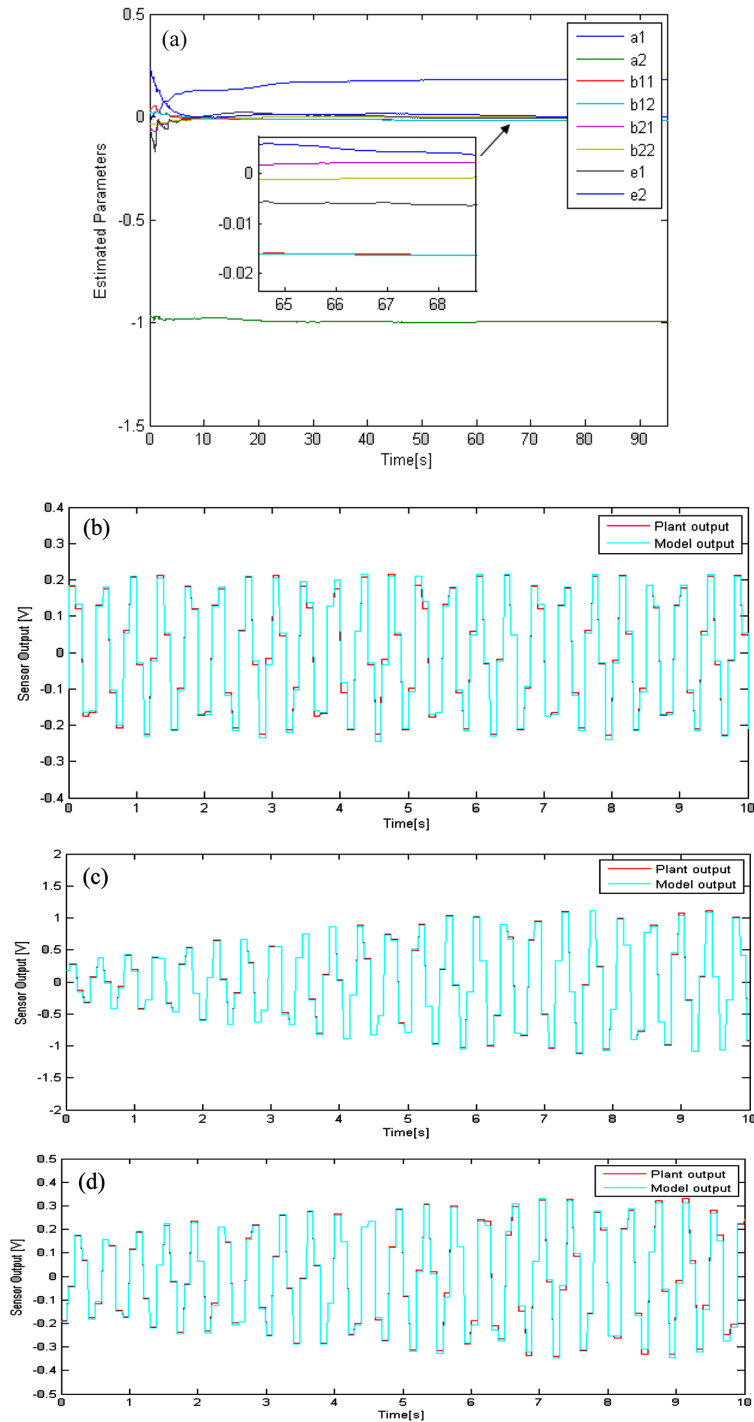


Fig. 3 Model validations for the second order system. (a) Parameter convergence, (b) comparison of output of the structure when excited through disturbance actuator, (c) comparison of output of the structure when excited through control actuator 1 and (d) comparison of output of the structure when excited through control actuator 2

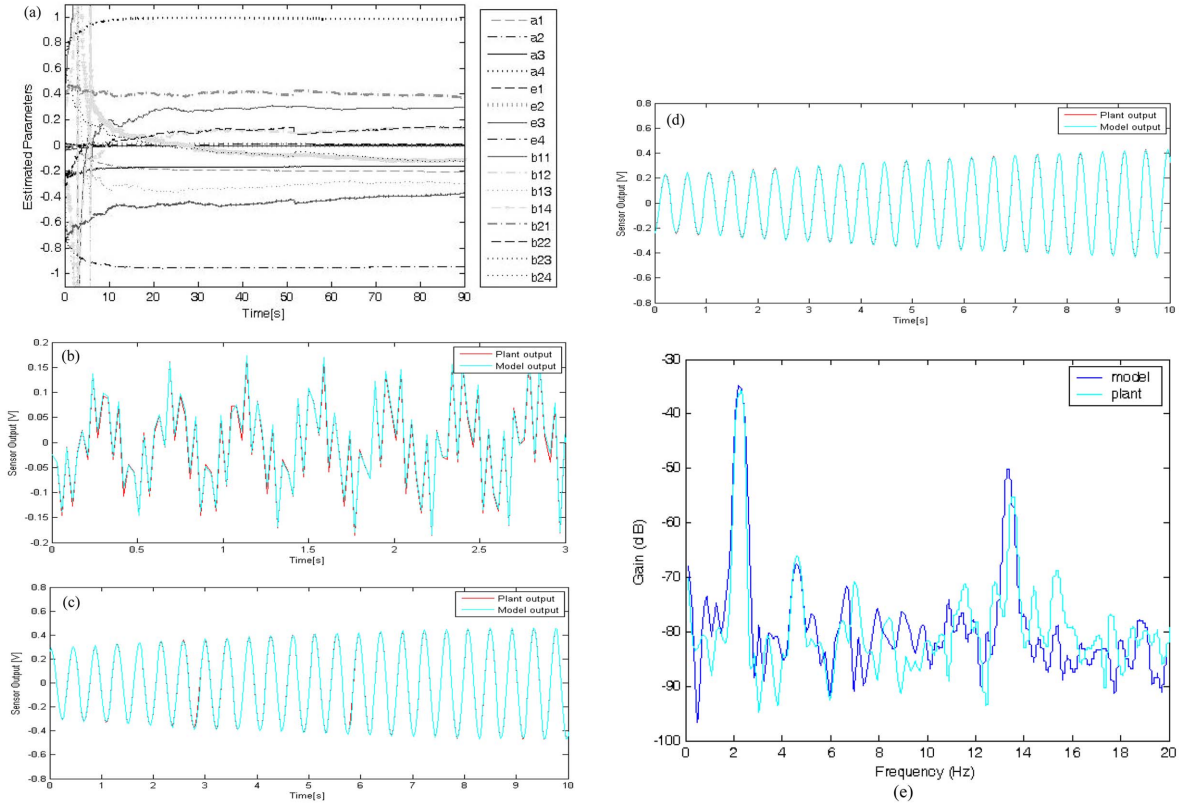


Fig. 4 Model validations for the fourth order system. (a) Parameter convergence, (b) comparison of output of the structure when excited through disturbance actuator, (c) comparison of output of the structure when excited through control actuator 1, (d) comparison of output of the structure when excited through control actuator 2, and (e) comparison of frequency responses of the structure

The model responses in time and frequency domain are found to match very closely with the actual structure response as seen from their comparison in Fig. 4.

4. Review of fast output sampling feedback control law

Consider a linear continuous-time invariant state space model

$$\dot{\mathbf{x}} = \mathbf{A}\mathbf{x} + \mathbf{b}u; y = \mathbf{C}^T\mathbf{x} \quad (11)$$

where $\mathbf{x} \in \mathfrak{R}^n$, $u \in \mathfrak{R}^m$, $y \in \mathfrak{R}^p$ and \mathbf{A} , \mathbf{b} and \mathbf{C}^T are constant matrices. It is assumed that $(\mathbf{A}, \mathbf{b}, \mathbf{C}^T)$ is controllable and observable. A discrete time invariant linear system is obtained by sampling the system in Eq. (1) at a sampling interval of τ . Now assume that output measurements are available, at the time instants $t = l\Delta$, where $l = 0, 1, 2 \dots$ and, the sampling interval τ is divided into N subintervals with $\Delta = \tau/N$ and N is equal to or greater than the observability index (ν) of the discrete system obtained by sampling the system in Eq. (11) at the rate of $1/\Delta$. The control law is illustrated in Fig. 5.

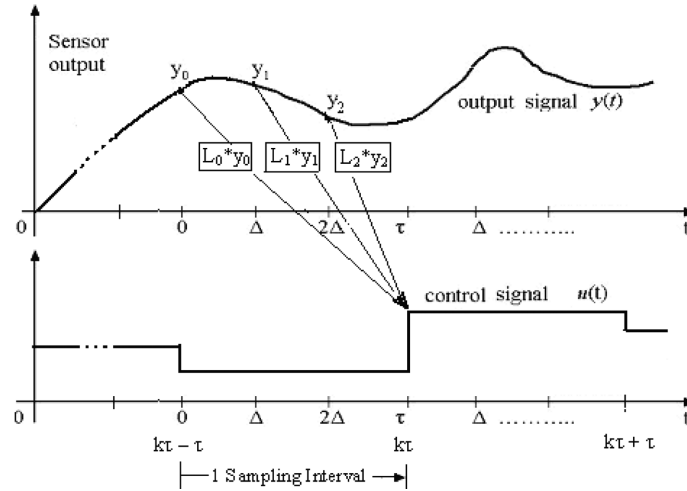


Fig. 5 Visualization of fast output sampling feedback control

The control signal $u(t)$ is then generated according to

$$u(t) = [L_0 \ L_1 \ \dots \ L_{N-1}] \begin{bmatrix} y(k\tau - \tau) \\ y(k\tau - \tau + \Delta) \\ \vdots \\ y(k\tau - \Delta) \end{bmatrix} \tag{12}$$

$$u(t) = \mathbf{L}y_k, \quad k\tau < t \leq (k+1)\tau$$

where the matrix blocks L_j represents output feedback gains.

Let $(\Phi_\tau, \Gamma_\tau, C^T)$, (Φ, Γ, C^T) be the system obtained by sampling the system $(\mathbf{A}, \mathbf{b}, C^T)$ at the rates of $1/\tau$ and $1/\Delta$.

Consider the discrete time system having at time $t = k\tau$, the input $u_k = u(k\tau)$, state $x_k = x(k\tau)$, the output y_k represented as

$$\mathbf{x}_{k+1} = \Phi_\tau \mathbf{x}_k + \Gamma_\tau u_k; \quad y_{k+1} = C_0 x_k + D_0 u_k \tag{13}$$

where

$$\mathbf{C}_0 = \begin{bmatrix} C^T \\ C^T \Phi \\ \vdots \\ C^T \Phi^{N-1} \end{bmatrix}; \quad \mathbf{D}_0 = \begin{bmatrix} 0 \\ C^T \Gamma \\ \vdots \\ C^T \sum_{j=0}^{N-2} \Phi^j \Gamma \end{bmatrix}$$

Now design a state feedback gain \mathbf{F} such that $(\Phi_\tau + \Gamma_\tau \mathbf{F})$ has no eigen values at origin and provides the desired closed loop behavior. For this state feedback one can define the fictitious measurement matrix

as $\mathbf{C}(\mathbf{F}, N) = (\mathbf{C}_0 + \mathbf{D}_0\mathbf{F})(\Phi_\tau + \Gamma_\tau\mathbf{F})^{-1}$, which satisfies the fictitious measurement equation $y_k = \mathbf{C}x_k$, then the feedback control in Eq. (12) can be interpreted as static output feedback $u_k = \mathbf{L}y_k$, for the system in Eq. (13) with the measurement matrix \mathbf{C} . To realize the effect of \mathbf{F} through \mathbf{L} , it must satisfy

$$\begin{aligned} \mathbf{x}_{k+1} &= (\Phi_\tau + \Gamma_\tau\mathbf{F})\mathbf{x}_k = (\Phi_\tau + \Gamma_\tau\mathbf{L}\mathbf{C})\mathbf{x}_k \\ \mathbf{L}\mathbf{C} &= \mathbf{F} \end{aligned} \quad (14)$$

For $N \geq v$, \mathbf{C} has full column rank, any state feedback gain can be realized by fast output sampling gain \mathbf{L} . If the initial state is unknown, there will be an error, $\Delta u_k = u_k - \mathbf{F}x_k$ in constructing a control signal under state feedback. It is then verified that the closed loop dynamics are governed by

$$\begin{bmatrix} x_{k+1} \\ \Delta u_{k+1} \end{bmatrix} = \begin{bmatrix} (\Phi_\tau + \Gamma_\tau\mathbf{F}) & \Gamma_\tau \\ \mathbf{0} & \mathbf{L}\mathbf{D}_0 - \mathbf{F}\Gamma_\tau \end{bmatrix} \begin{bmatrix} x_k \\ \Delta u_k \end{bmatrix} \quad (15)$$

The system in Eq. (13) is stable, iff \mathbf{F} stabilizes (Φ_τ, Γ_τ) and matrix $(\mathbf{L}\mathbf{D}_0 - \mathbf{F}\Gamma_\tau)$ has all its eigen values inside the unit circle.

5. Design of the fast output sampling feedback controller

The fast output sampling feedback control scheme to suppress the amplitude of the vibration at resonance of an SMA actuated cantilever beam is designed and simulated. The design involves control of the first mode of vibration using the second order model and the first two modes of vibration using the fourth order model.

5.1 Design for the second order system

Let $(\Phi_\tau, \Gamma_\tau, \mathbf{C}^T)$ be the discrete time system obtained by sampling the system in Eq. (9) at a rate of $1/\tau$, τ is 0.1 second.

Stabilizing state feedback controllers are designed for the system with actuator 1 and actuator 2 such that the eigen values of $(\Phi_\tau + \Gamma_{\tau 1}\mathbf{F}_1)$ and $(\Phi_\tau + \Gamma_{\tau 2}\mathbf{F}_2)$ are not at the origin. The controller gains are $\mathbf{F}_1 = [-12.0296 \ 20.6519]$ and $\mathbf{F}_2 = [-12.6081 \ 18.9854]$. To assess the performance of the state feedback controller in simulation, a sinusoidal signal of amplitude 1 volt peak to peak at first mode frequency is applied as excitation input through the disturbance actuator. The output of the controller 1 (\mathbf{F}_1) is applied for 1 second to the actuator 1, then the control is switched over to controller 2 (\mathbf{F}_2) which applies its output to actuator 2 for the next 1 second. The repetition of switching between actuators allows them to actuate and cool alternatively. Control signal is applied continuously to the system by this approach, in spite of the limitations of the individual actuators in terms of heating and cooling. The open loop response, response with the state feedback controller and the control signal obtained through simulation are shown in Fig. 6.

The observability index of the system $(\Phi_\tau, \Gamma_\tau, \mathbf{C}^T)$ is 2. Let $(\Phi, \Gamma, \mathbf{C}^T)$ be the discrete time system obtained by sampling $(\mathbf{A}, \mathbf{b}, \mathbf{C}^T)$ at a rate of $1/\Delta$ where $\Delta = \tau/N$ and the number of subintervals N is chosen as 4. The sampling time Δ of the $(\Phi, \Gamma, \mathbf{C}^T)$ system is 0.025 s.

To realize the state feedback gains \mathbf{F}_1 and \mathbf{F}_2 by output feedback gains \mathbf{L}_1 and \mathbf{L}_2 , the equation

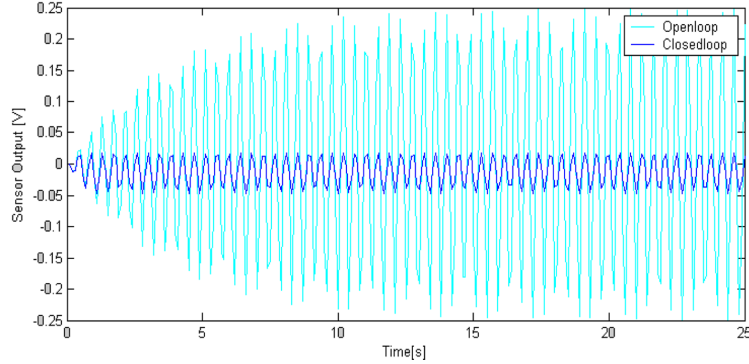


Fig. 6 Uncontrolled and controlled responses with state feedback gain

$\mathbf{L}_1\mathbf{C}_1 = \mathbf{F}_1$ and equation $\mathbf{L}_2\mathbf{C}_2 = \mathbf{F}_2$ are solved using Linear Matrix Inequalities (LMIs). The fast output sampling feedback gains obtained as explained above are

$$\mathbf{L}_1 = [22.9598 \quad -31.1691 \quad -31.1460 \quad 22.2747] \text{ and}$$

$$\mathbf{L}_2 = [22.1643 \quad -32.3060 \quad -31.5226 \quad 23.6424]$$

The open loop response, response with fast output sampling feedback gain and the control signal obtained through simulation are shown in Fig. 7.

To obtain a better appraisal of the usefulness of the control performance, the structure is subjected to broadband excitation. The simulation results for the second order system subjected to broadband excitation of 2 volt peak to peak and swept over the frequency range of 0 to 5 Hz is shown in Fig. 8.

5.2 Design for the fourth order system

The discrete time system obtained by sampling the system in Eq. (10) at 0.02 second is

$$x(k+1) = \Phi_\tau x(k) + \Gamma_\tau u(k) + \mathbf{E}_\tau d(k)$$

$$y(k) = \mathbf{C}^T x(k)$$

Stabilizing state feedback gains are designed and applied in accordance with the Section 5.1. The gains with actuator 1 and actuator 2 are

$$\mathbf{F}_1 = [-8.6151 \quad -9.1544 \quad 12.9835 \quad -22.1376] \text{ and}$$

$$\mathbf{F}_2 = [9.7655 \quad -10.4589 \quad 11.2083 \quad -18.6212]$$

The performance of the controller is carried out through simulation by applying a sine wave disturbance of amplitude 1 volt peak to peak. Initially the structure is excited with the first mode frequency and then with the second mode frequency as shown in Fig. 9(a). The open loop response and response with the state feedback gain obtained through simulation are shown in Fig. 9(b).

To realize the state feedback gains \mathbf{F}_1 and \mathbf{F}_2 by output feedback gains \mathbf{L}_1 and \mathbf{L}_2 , the LMIs are solved for $N = 4$. The fast output sampling feedback gains obtained are

$$\mathbf{L}_1 = [-218.1208 \quad 659.3829 \quad -604.4293 \quad 183.5668] \text{ and}$$

$$\mathbf{L}_2 = [-61.6476 \quad 169.1996 \quad -88.9937 \quad -1.2916]$$

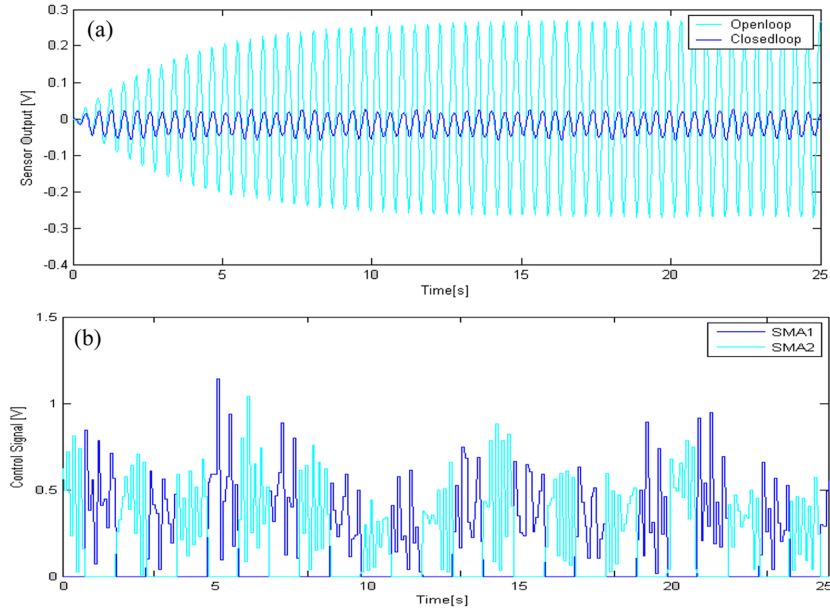


Fig. 7 Responses with fast output sampling feedback controller (simulation): (a) Uncontrolled and controlled and (b) control signal

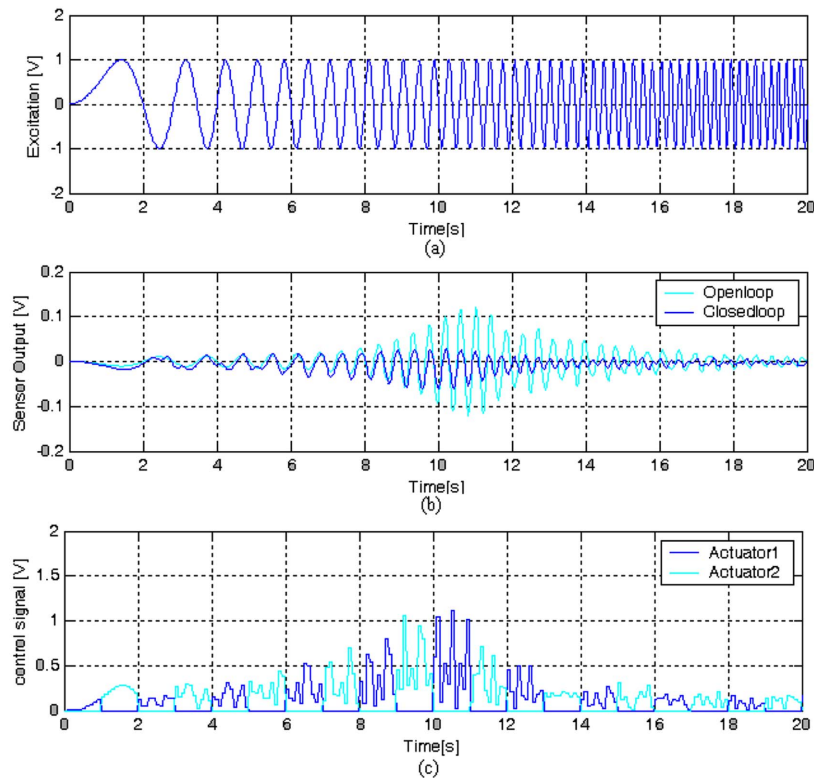


Fig. 8 Responses with fast output sampling feedback controller (simulation) with sweep signal: (a) Sweep signal, (b) uncontrolled and controlled and (c) control signal

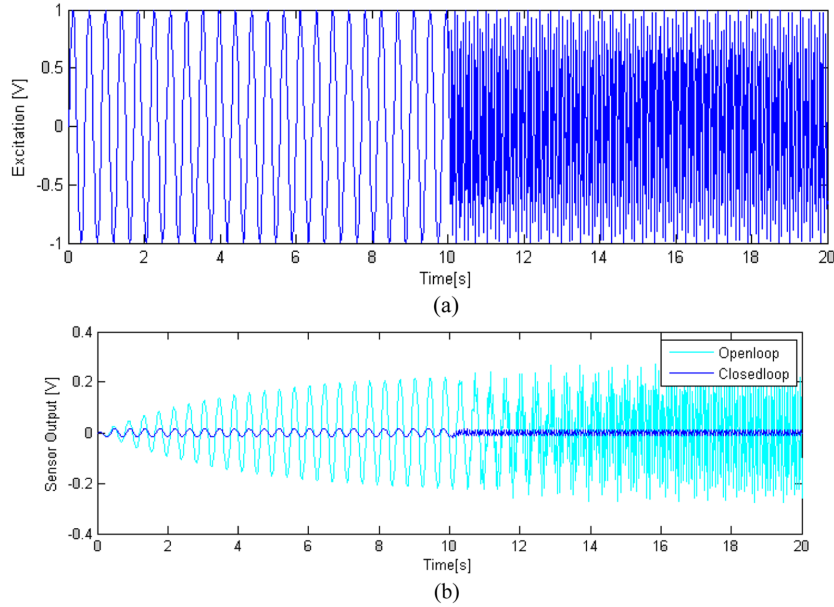


Fig. 9 Responses with state feedback controller: (a) Excitation changes from first to second natural frequency and (b) uncontrolled and controlled

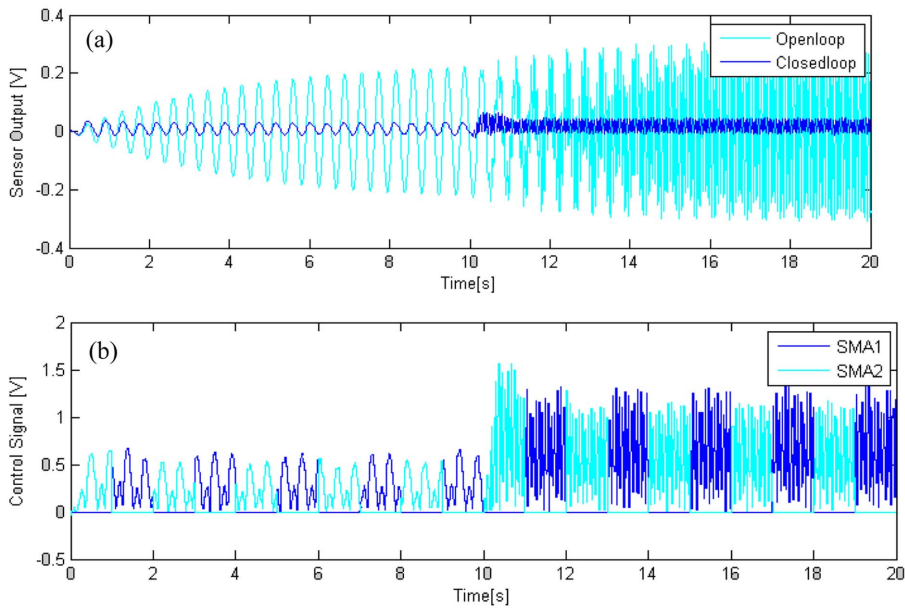


Fig. 10 Responses with fast output sampling feedback controller (simulation): (a) Uncontrolled and controlled and (b) control signal

The open loop response, response with fast output sampling feedback control and the control signal obtained through simulation are shown in Fig. 10. The performance of the controller to broadband excitation is evaluated through simulation for a sweep signal excitation of 2 volt peak to peak swept over the frequency range of 0 to 25 Hz, respective results are shown in Fig. 11.

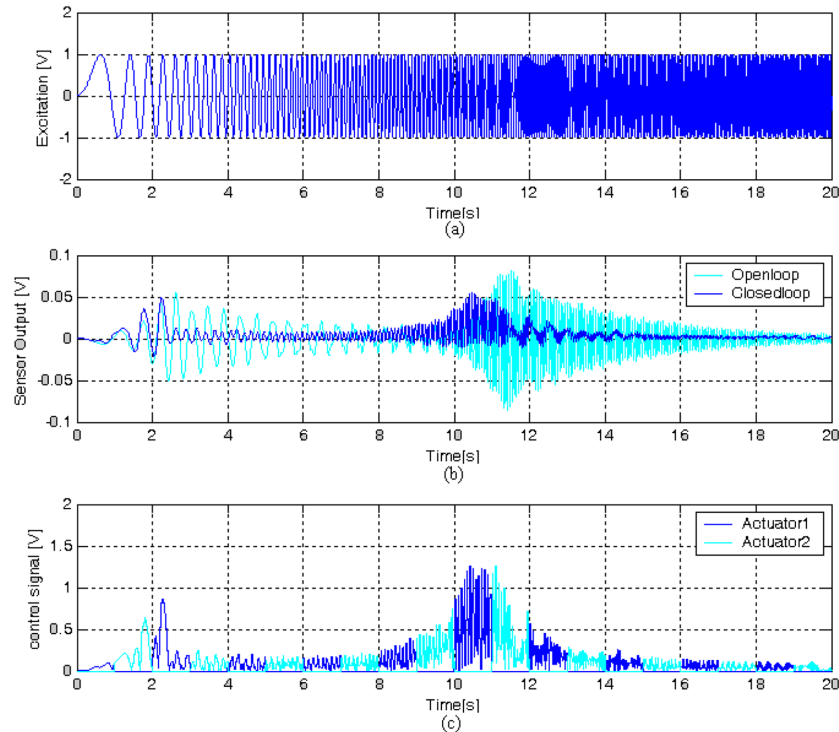


Fig. 11 Responses with fast output sampling feedback controller (simulation) with sweep signal: (a) Sweep signal, (b) uncontrolled and controlled and (c) control signal

6. Experimental implementation

Evaluation of the performance of the controller through experiment is an essential part of the design. To substantiate the design and simulation results the controller designed for the second order system is implemented using the experimental facility shown in Fig. 1. The structure is made to vibrate at its first mode frequency (2.36 Hz) by applying a sinusoidal excitation signal of 1 volt peak to peak to the disturbance actuator from an arbitrary waveform generator (Agilent 33220A). As required by the fast output sampling feedback control the sensor output is sampled at 0.025 second ($\Delta = \tau/N$) through the ADC port of dSPACE and MATLAB/SimulinkTM. The control signal is updated at every 0.1 second (τ), while it is applied to the actuator only at alternate 1 second. The control signal generated by the controller 1 is applied to actuator 1 at alternate 1 s while the control signal generated by controller 2 is applied to actuator 2 at the other alternate 1 second. Switching between the controllers is cycled at every consecutive period of 1 second, while continuous actuation is provided to the system by the alternate actuators.

The controller is implemented by developing a real time SimulinkTM model using MATLAB RTW. The open loop response, closed loop response with fast output sampling feedback control and control signal are shown in Fig. 12. The frequency response of the system is acquired using Digital Storage Oscilloscope (Agilent 54621A) and is shown in Fig. 13.

To demonstrate the effectiveness of the control design to broadband excitation, the structure is

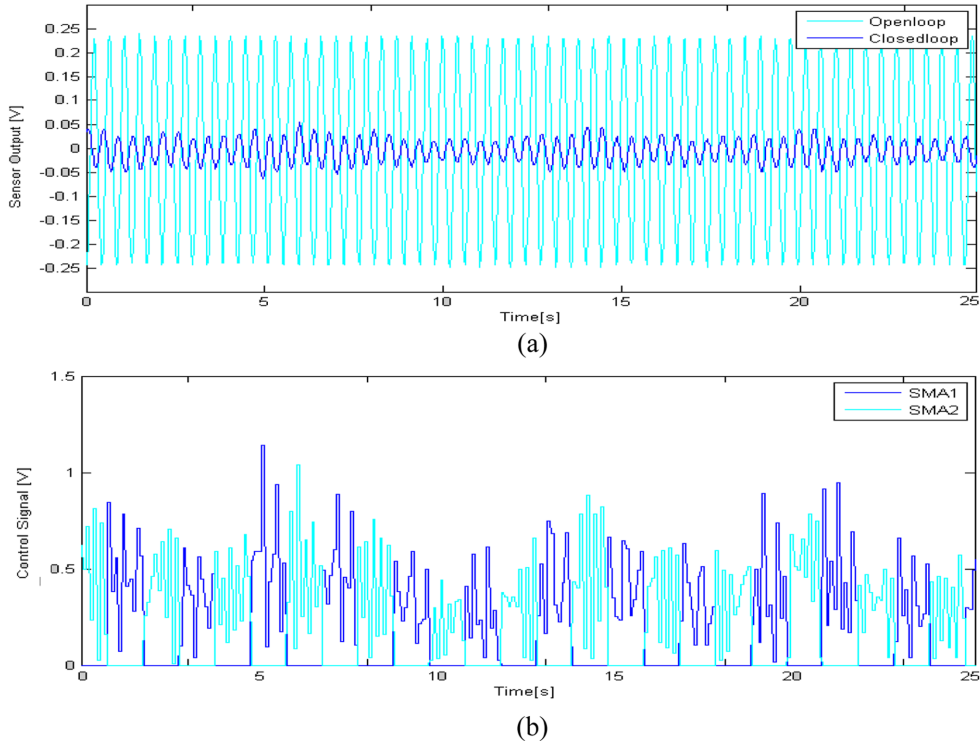


Fig. 12 Experimental results with fast output sampling controller: (a) Uncontrolled and controlled and (b) control signal

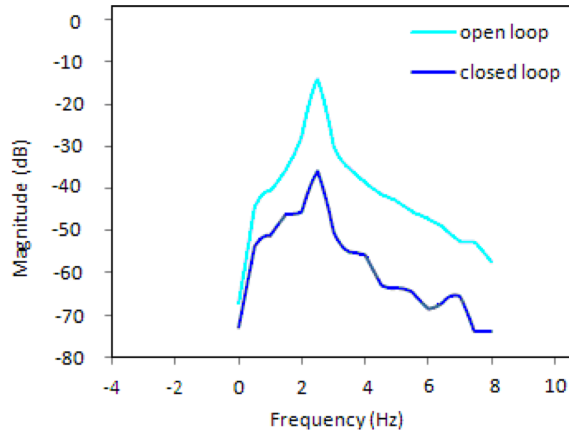


Fig. 13 Frequency responses with and without fast output sampling controller

made to vibrate by applying a sinusoidal sweep excitation signal of 4 volt peak to peak over the frequency range of 0 to 25 Hz to the disturbance actuator from the arbitrary waveform generator. The corresponding broadband excitation, open loop response, closed loop response with fast output sampling feedback control and control signal are represented in Fig. 14.

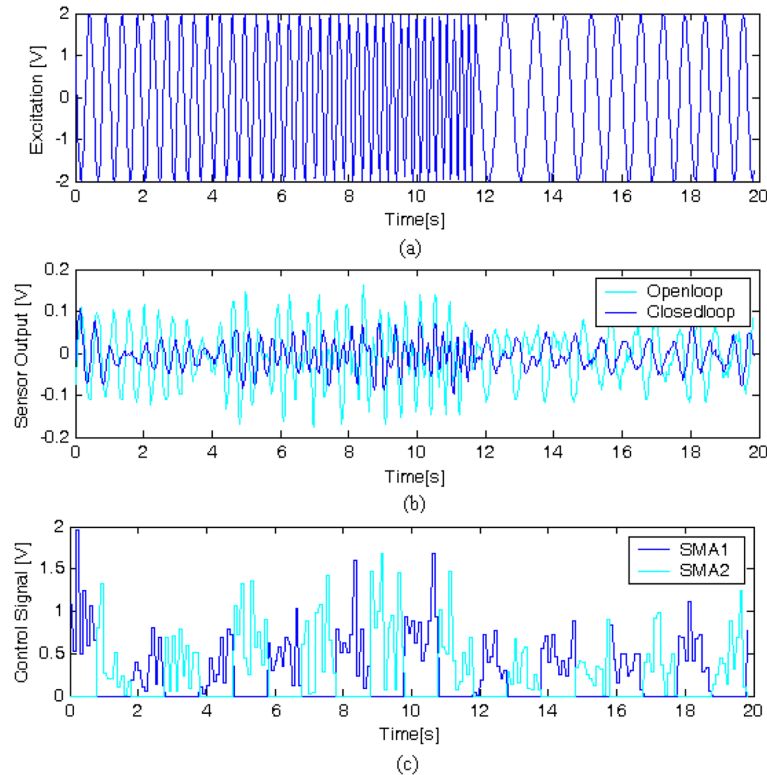


Fig. 14 Frequency responses with and without fast output sampling controller

7. Conclusions

The second order and fourth order models of SMA actuated and piezoelectric sensed cantilever beam structure excited at its natural frequency (resonance) have been identified using online ARX RLS system identification approach.

The fast output sampling feedback controller is designed and simulated for the system models. The state feedback gain \mathbf{F} is realized by means of the output feedback gain \mathbf{L} by lifting the measurement matrix (fictitious). State feedback gain \mathbf{F} is designed to provide the desired closed loop behaviour by placing the eigen values within the unit circle other than at the origin, hence the FOS feedback always guarantees the stability of the closed loop system when compared to the output feedback control. It represents the simplest closed loop control that can be realized in practice. Even though the controller is derived using state feedback gain \mathbf{F} , estimation of the states is not required for implementing the controller, but only the plant output is required for implementation. As the fast output sampling feedback gains are computed from the state feedback gains the closed loop responses obtained through simulation with output feedback gains closely matches with that of the state feedback gains for the systems. The closeness depends on the selection of LMI variables. For a sinusoidal excitation of 1 volt peak to peak an uncontrolled response of 0.225 V peak to peak is obtained. In the problem of first mode vibration control, reduction of 88% is obtained through simulation and 87% reduction is obtained experimentally.

Control signal required for this reduction is 0.75 V both in simulation and experimentally. The simulation results of the fourth order system gives a reduction of 90% of vibration at the first and the second mode. Control signal required for this reduction is 0.55 V at the first and 1.1 V at the second mode.

This work demonstrates the effectiveness of the control design to broadband excitation; the structure is made to vibrate by applying a sinusoidal sweep excitation signal from 0 Hz to the frequency that is at least twice the resonant frequency of the model and respective response is obtained indicating successful vibration suppression at the first two modes considered. The simulation and experimental results demonstrate the performance and practical simplicity of the controller.

References

- Baz, A. Imam, K. and McCoy, J. (1990), "Active vibration control of flexible beams using shape memory actuators", *J. Sound. Vib.*, **140**(3), 437-456.
- Bu, X., Ye, L., Su, Z. and Wang, C. (2003), "Active control of a flexible smart beam using a system identification technique based on ARMAX", *Smart. Mater. Struct.*, **12**(5), 845-850.
- Choi, S.B. and Cheong, C.C. (1996), "Vibration control of a flexible beam using shape memory alloy actuators", *J. Guid. Control. Dynam.*, **19**(5), 1178-1180.
- Ezhilarasi, D., Umapathy, M. and Bandyopadhyay, B. (2006), "Design and experimental evaluation of piecewise output feedback control for structural vibration suppression using PZT patches", *J. Smart Mater. Struct.*, **15**(6), 1927-1938.
- Ljung, L. (1999), *System Identification theory for the user*, Prentice Hall PTR, New Jersey.
- Seelecke, S. and Muller, I. (2004), "Shape memory alloy actuators in smart structures: Modeling and simulation", *Appl. Mech. Rev.*, **57**(1), 23-46.
- Sohn, J.W., Han, Y.M. and Choi, S.B. (2009), "Vibration and position tracking control of flexible beam using SMA wire actuators", *J. Vib. Control.*, **15**(2), 263-281.
- Song, G., Ma, N. and Lee, H. (2007), "Position estimation and control of SMA actuators based on electrical resistance measurement", *Smart Struct. Syst.*, **3**(2), 189-200.
- Srinivasan, A. and McFarland, D. (2001), *Smart Structure: Analysis and Design*, Cambridge University Press.
- Waram, T. (1993), *Actuator design using Shape Memory Alloys*, Mondotronics, Inc., Canada.
- Werner, H. and Furuta, K. (1995), "Simultaneous stabilisation based on output measurements", *Kybernetika*, **31**(4), 395-411.